JOURNAL OF MATERIALS SCIENCE 30 (1995) 3440–3448

Development, preliminary testing and future applications of a rational correlation for the grain densities of vapour-deposited materials

T. KHO, J. COLLINS, D. E. ROSNER
Yale University, Department of Chemical Engineering, High Temperature Chemical Reaction Engineering (HTCRE) Laboratory, New Haven, CT 06520–8286, USA

It is conjectured and found in this work that the grain densities (suitably normalized) of vapour-deposited solid materials depend principally on competition between the successful arrival rate of their reagent molecules and the surface diffusion rate of admolecules on their growing surfaces. The ratio of these two rates defines an important dimensionless Damköhler number, called here the "burial" parameter, β. Available grain density data for seven vapour deposited materials [silicon (Si), gallium arsenide (GaAs), silicon carbide (SiC), silicon nitride (Si_3N_4), titanium oxide (TiO_2), boron nitride (BN) and graphite (C)] are used to establish and test the "universality" of the proposed *normalized grain density versus burial parameter correlation*. As anticipated, these data show that the normalized grain densities of these materials increase with their corresponding burial parameters. Moreover, for estimated burial parameters much less than unity, the deposits formed are indeed reported to be amorphous, while the deposits are observed to be crystalline under conditions for which $\beta \gg 1$ is estimated. As the burial parameter decreases, the reported grain densities of turbostratic, "layered", materials are found to decrease more gradually than for materials with no turbostratic structure. While the present implementation of this basic hypothesis cannot be regarded as "complete", it is argued that a rationally-based, reasonably "universal" vapour deposit density correlation of this general form can be quite useful in making rational predictions of deposit quality. Moreover, it appears that this path to such mechanistically plausible correlations, which, using available experimental data, can be implemented/tested even in the absence of a "complete" theory, can be broadened to include other important deposit characteristics *via* the introduced of additional characteristic time ratios.

1. Introduction

1.1. Vapour deposition of solids

In the course of research and development on processes for depositing solid films or objects from the vapour phase, a very rich literature on deposit properties under various experimental conditions has been accumulated. However, what seems to be missing from most, if not all of the vapour deposition literature, including those giving interesting experimental results on deposit microstructure–properties versus reactor conditions, are rational correlations in terms of relevant physicochemical dimensionless groups, such as Damköhler type ratios of relevant characteristic times, commonly used in the chemical reaction engineering literature [1].

1.2. Goals

Developed and demonstrated here is a rational, non-dimensional correlation procedure that can be used to predict grain densities for deposits grown from the vapour phase. Such a correlation, which should be "universal", has long been needed and could, if successful, be used to guide the selection and mathematical analysis of vapour deposition conditions required for the growth of materials with desired properties [2] at acceptable rates. Moreover, as mentioned in the conclusions, it seems likely that, by introducing other relevant dimensionless time ratios in future work, additional properties of vapour deposits, e.g. grain size and shape, deposit porosity, bulk density, etc., could be anticipated for use in more comprehensive transport modelling of chemical (and physical) vapour deposition systems.

2. Experimental procedure

2.1. A "burial" parameter

Over a range of vapour deposition conditions, very different deposit microstructures have been observed via analytical methods such as X-ray diffraction (XRD) spectroscopy and scanning electron

0022–2461

microscopy. Several researchers [3–5] have made (but evidently not sufficiently implemented or exploited) the plausible suggestion that the microstructure of a vapour deposited material (whether amorphous or crystalline) should be related to the ability of its incident atoms–molecules to find their way to the correct crystal sites by surface diffusion before being "buried" by subsequent depositing atoms/molecules. This ability is dependent upon the competition between the successful arrival rate of depositing molecules on the growing film and the surface diffusion rate of the admolecules. It is conjectured and shown in this preliminary work that the normalized grain densities of previously studied vapour deposited materials can be successfully correlated using the ratio of these two rates, which is estimated below for a variety of solids and experimental growth conditions. In the spirit of chemical reaction engineering [1], this ratio defines a crucial dimensionless Damköhler number which, for convenience, shall be called the "burial" (really 'burial avoidance') parameter, β.

2.1.1. Evaluation of the relevant "burial parameter" and basic assumptions

Explicitly, the burial parameter, β, is defined here as the ratio of the characteristic time, t, for successful arrival of a reactant molecule on the deposit surface to the characteristic time for an adsorbed atom or molecule to surface diffuse to a crystal lattice position. Alternately, this parameter can also be viewed and expressed as a ratio of the surface diffusion frequency, f, of admolecules ($f_{\text{surface diffusion}} = t^{-1}_{\text{surface diffusion}}$) to the successful arrival rate of depositing molecules on the growing film ($f_{\text{successful arrival}} = t^{-1}_{\text{successful arrival}}$), i.e.

"Burial" parameter, $\beta \equiv$

$$\frac{t_{\text{successful arrival}}}{t_{\text{surface diffusion}}} = \frac{f_{\text{surface diffusion}}}{f_{\text{successful arrival}}} \qquad (1)$$

The procedures for estimating the relevant β values over a wide variety of experimental vapour deposition conditions for which deposit density data are available will be presented below.

The basic conjecture is that if available density data for vapour deposited materials, suitably normalized, are recast in this form, the grain densities of any such material will increase systematically as its burial parameter, β, increases. Thus, for burial avoidance parameters much less than unity, $\beta \ll 1$, the deposits should be low density amorphous solids, while deposits should be dense and crystalline if grown under conditions where the burial avoidance parameter is much greater than unity, $\beta \gg 1$. This hopefully "universal" burial parameter hypothesis, to be tested and illustrated below, is of course, not free of certain assumptions about the vapour deposition systems to which it can be applied:

1. Deposition of the solid film is attained strictly via a vapour–solid growth process and is not modified by homogeneous chemical reaction and nucleation in the vapour phase [6]. Clearly, microparticles produced in the vapour phase will usually have a different morphology than a film deposited exclusively by heterogeneous nucleation and, their random incorporation would normally lower the density of a "codeposited" film. Thus, the grain density correlation should be, and will be, tested only under experimental conditions for which particle nucleation/growth in the vapour phase can be safely precluded.

2. During deposition, the microstructure of the as-deposited film is not subsequently modified by any solid state transformation associated with the rearrangement of atoms in the solid deposit. These longer time scale solid state transformations include the (partial) crystallization of initially amorphous film and subsequent grain growth.

3. Whether the deposits under consideration are crystalline or amorphous, their microstructure is assumed to be homogeneous throughout the deposit. Thus, a decrease in grain densities is considered to be due to a continuous increase of disorder in the arrangement of their constituent atoms, rather than the existence of a heterogeneous structure composed of a mixture of both the amorphous and crystalline "patches".

4. The crystal density of the material being deposited is considered to be higher than its amorphous (glassy) density. Although most materials (including the seven explicitly examined below) obey this "rule", there are some familiar exceptions, e.g. H_2O in its crystalline state (ice) has a density of about 10% lower than its amorphous state (water).

If the abovementioned "complications" are not present, here it is investigated whether available grain density data, when recast as a ratio of density differences: $(\rho_{\text{grain}} - \rho_{\min})/(\rho_{\max} - \rho_{\min}) \equiv \mathscr{R}$ (see Equation 8 below), can be correlated in accord with the burial parameter hypothesis presented.

2.1.2. Successful arrival rate of depositing molecules

For a simple chemical vapour deposition (CVD) system: A(g) + B(g) → AB(s), the flux, f'', of a depositing vapour species say, A(g), on a surface can be written, from simple kinetic theory as follows [4]

$$f''_{\text{A, successful arrival}} = \frac{\alpha p_{\text{A},w}}{(2\pi M_{\text{A}} k_{\text{B}} T)^{1/2}} \qquad (2)$$

On the area of, say, one lattice site, A_l, this flux corresponds to the rate

$$f_{\text{A, successful arrival}} = \frac{\alpha p_{\text{A},w} A_l}{(2\pi M_{\text{A}} k_{\text{B}} T)^{1/2}} \qquad (3)$$

In these relations, α is the experimentally inferred fraction of A(g) incident on the substrate surface which leads to chemical reaction–incorporation, $p_{\text{A,w}}$ is the partial pressure of reagent A(g) near the vapour–solid interface, M_{A} is the molecular mass of A, while k_{B} is the Boltzmann constant. The area associated with one lattice site, A_l is here taken to be the area of a unit cell in the preferred orientation plane of

the film divided by the number of A atoms in that area. Since amorphous materials are structureless, they do not display any preferred orientation and have no fixed lattice parameters. Accordingly, their A_l values were simply taken to be the same as those of their most stable crystalline counterparts deposited from the vapour phase.

The important rate $f_{A,\text{successful arrival}}$ can also be written in terms of the frequently reported deposition rate of AB(s), $\dot{r}''_{AB}$ (in units of mole per unit area per unit time) as shown below

$$f_{A,\text{successful arrival}} = \dot{r}''_{AB} A_l N_A \quad (4)$$

where N_A is Avogadro's number.

2.1.3. Surface diffusion rate of admolecules

The surface diffusion coefficient for the relevant admolecules on a vapour-deposited film is not only dependent upon the surface temperature of the film but also on two important parameters, namely the activation energy for surface diffusion, ΔE_{SD}, and the vibrational frequency, ν_0, of admolecules on the deposit surface. ΔE_{SD} is the energy barrier that the adsorbed atoms–molecules need to overcome in order to move or surface diffuse (SD) to other surface sites. The rate at which an adsorbed atom–molecule surface diffuses from one discrete site to another can be expressed in the Arrhenius ("activated") form [4], as shown in Equation 5

$$f_{\text{surface diffusion}} = \nu_0 \exp(-\Delta E_{SD}/RT) \quad (5)$$

The relationship between the frequently reported absorption or emission wavelength of the electromagnetic spectrum, λ_0, and its corresponding frequency, ν_0 [7], is of course

$$\nu_0 = \left(\frac{c}{\lambda_0}\right) \quad (6)$$

where c is the speed of light in vacuum.

The natural vibrational frequencies of atoms in molecules and in crystals fall in the infrared (i.r.) range [8]. Admolecules on a deposit surface also vibrate at some characteristic i.r. frequency. To estimate the burial parameter associated with a particular deposit, it is necessary to identify what the diffusing species are* and assign appropriate ν_0 and ΔE_{SD} values. However, for CVD systems, the actual diffusing species are usually not probed directly and, hence, are almost inevitably a matter of some conjecture. Yet, due to the narrow range of i.r. absorption wavelengths for materials, the i.r. vibrational frequencies for many materials and admolecules are of the order of $10^{13}\ s^{-1}$. Thus, almost regardless of the identity of the diffusing species on a deposit surface, the differences between their i.r. vibrational frequencies are not considered significant and, as noted below, uncertainties due to this cause will be negligible compared to uncertainties associated with ΔE_{SD}.

2.1.4. Estimation of the activation energy for surface diffusion of admolecules

The activation energy for surface diffusion, ΔE_{SD}, is the most important parameter needed to predict the surface diffusion rate of admolecules from which to estimate the corresponding burial parameter. Unfortunately, ΔE_{SD} is not readily available in the literature for most vapour deposition systems. Below are some sources–methods used to estimate the appropriate value of the activation energy for surface diffusion.

1. Literature: The values of the activation energy for self surface diffusion of certain materials are available in the literature. Most experiments and associated models developed to estimate this activation energy are only applicable under stringent conditions and require the values of additional parameters not readily available. For example, the step–flow crystal growth model illustrated by Henderson and Helm [9] to estimate the activation energy for self surface diffusion of silicon requires the value of parameters like the activation energy for adatom desorption and accurate reagent concentrations near the substrate surface at various deposition temperatures.

2. Dryburgh's method for covalent crystals [4]: Dryburgh [4], proposed methods for estimating the activation energy for surface diffusion of covalent (zincblende structure), ionic and metallic crystals. Indeed, he presented such estimates for 33 crystals, including group IV elements, III–V compounds, ionic solids and metals. The agreement of these estimates with experimental results was shown to be satisfactory for silicon (Si), germanium (Ge), gallium arsenide (GaAs), indium phosphide (InP) and cadmium telluride (CdTe), all of which are covalent crystals. Since Dryburgh has only been able to establish confidence for his covalent crystal results, only his covalent crystal model was used for estimating the activation energy for surface diffusion in this work. Dryburgh [4] suggested that in the case of an AB compound of zincblende structure, the position of an adsorbed atom with respect to the surface may be considered as being determined completely by the highly directional nature of a single sp^3 bond. Therefore, any lateral movement of the atom during surface diffusion can take place only if this single bond is effectively broken. Hence, the activation energy for surface diffusion, E_{SD}, is the energy required to break a single bond between an A (or a B) atom and solid AB and can be estimated from thermochemical data, i.e. the heat of formation of the crystals and the heat of atomization of their constituent elements.

3. Estimation of the activation energy for surface diffusion by setting the burial parameter to unity, $\beta = 1$, for a deposit which is shown by XRD patterns to be in transition between its amorphous and

* There is, of course, less ambiguity in what the diffusing species are for physical vapour deposition (PVD) than for CVD (PVD involves no chemical reaction which may lead to the generation of many additional species). Thus, in future work, better ν_0 assignments may be possible for PVD systems.

crystalline state: This method of estimating the activation energy for surface diffusion is based on the burial parameter hypothesis itself. It was indeed Dryburgh's premise [4] that when β is equal to unity, the corresponding deposition temperature is near the minimum growth temperature required for crystals to be grown from the gas phase. Hence, by setting β equal to unity for a deposit shown by, say, XRD patterns to be in transition between its amorphous and crystalline state, the activation energy for surface diffusion of this deposit can be estimated from Equation 7 below. Thus, for $\beta = 1$

$$f_{\text{successful arrival}} = f_{\text{surface diffusion}}$$

so that E_{SD} can be estimated from

$$\dot{r}''_{AB} A_l N_A = \nu_0 \exp(-\Delta E_{SD}/RT) \quad (7)$$

where all properties are evaluated at the "transition density" growth conditions.

2.1.5. Selection and evaluation of an appropriate grain density variable

Since the ("escape-from-burial") parameter β is dimensionless, the grain density, ρ_{grain}, with which it is associated, is here made non-dimensional and normalized as follows:

Normalized grain density (difference):

$$\mathscr{R} \equiv \frac{\rho_{grain} - \rho_{min}}{\rho_{max} - \rho_{min}} \quad (8)$$

The maximum grain density, ρ_{max}, appearing in the denominator of $\mathscr{R}$ is presumed here to be the theoretical single crystal density, $\rho_{crystal}$. Conversely, the minimum grain density, ρ_{min}, is taken to be the lowest observed amorphous density of the material. Of course, "grains" do not exist in amorphous deposits, so the term "grain density" for such deposits is defined here as the solid density due to the random arrangement of the constituent atoms, and not due to the presence of any large scale porosity in the deposit. Here we neglected changes in ρ associated with the isobaric volume expansivity of these solids.

There are seven vapour deposited solids of primary interest to this work, because of the considerable amount of experimental data available in the literature which can be exploited to test and implement the proposed burial parameter–normalized density correlation, $\mathscr{R}(\beta)$. These materials are: silicon (Si), gallium arsenide (GaAs), silicon carbide (SiC), silicon nitride (Si_3N_4), titanium oxide (TiO_2), boron nitride (BN) and graphite (C).

Table I summarizes the important properties necessary to estimate the burial parameter for these seven materials. Lattice constants (a_0 and c_0) were obtained from Wyckoff [10] unless otherwise mentioned. Also, which method was used to estimate the activation energy for surface diffusion, ΔE_{SD}, is identified. Table II gives a summary of the various systems from which data have been used in a preliminary test of the burial parameter hypothesis. ΔE_A is the activation energy for

TABLE I Summary of properties necessary for estimating the burial parameter for the seven vapour deposited materials examined in this work

Material	Molecular mass ($g\,mol^{-1}$)	Crystal structure	Lattice constant (nm)	Crystal density ($g\,cm^{-3}$)	Amorphous density ($g\,cm^{-3}$)	ν_0 ($1\,s^{-1}$)	ΔE_{SD} ($kJ\,mol^{-1}$)	Method for ΔE_{SD}
Silicon	28.086	Diamond [4]	$a_0 = 0.543\,106\,26$ [11]	2.3290 [11]	1.7 [11]	1.260×10^{13} [12]	106 [13]	1
GaAs	144.642	Zincblende [14]	$a_0 = 0.565\,325$	5.1376 [12]		8.765×10^{12} [12]	106 [15]	1
β–SiC	40.097	Zincblende [16]	$a_0 = 0.435\,96$	3.2120 [16]	2.7 [17]	2.512×10^{13} [12]	193 [4]	2
α–Si_3N_4	140.285	Hexagonal [16]	$a_0 = 0.7753$	3.1840 [16]	2.6 [18]	2.518×10^{13} [19]	330 [18, 20]	3
			$c_0 = 0.5168$					
TiO_2 anatase	79.879	Tetragonal [21]	$a_0 = 0.3785$	3.8400 [22]	3.2 [23]	1.979×10^{13} [24]	145 [21, 25]	1&3
			$c_0 = 0.9514$					
BN	24.82	Hexagonal [26]	$a_0 = 0.2531$	2.2700 [26]	1.5	3.927×10^{13} [26]	310 [27, 28]	3
			$c_0 = 0.6661$					
Graphite	12.011	Hexagonal [26]	$a_0 = 0.2456$	2.2660 [29]	1.5 [29]	4.497×10^{13} [30]	96 [31]	1
			$c_0 = 0.6696$					

TABLE II Summary of the vapour deposition systems used to test the burial parameter correlation

Material	Reference	Process	Chemicals	P_{tot} (kPa)	Temperature (K)	ΔE_A (kJ mol^{-1})	Substrate	Deposit (single crystal or polycrystals or amorphous	PO[a]
Silicon	[9]	CVD[b]	SiH_4	0.003–0.020	1096–1256	84	Si(1 1 1)	Single	[1 1 1]
Silicon	[32]	CVD	SiH_4		973–1473	71	Si(1 1 1)	Single & poly	[1 1 1]
Silicon	[33]	CVD	SiH_4		1348–1498		Si(1 1 1)	Single & poly	[1 1 1]
Silicon	[34]	Vacuum evaporation	P-doped Si	UHV[h]	RT[i]		Gold electrode	Amorphous	
GaAs	[35]	MOCVD[c]	AsH_3–TMG[d]	101.325	723–1323	54	GaAs(1 0 0)	Single	[1 0 0]
GaAs	[36]	MOCVD			1023–1108	84	GaAs(0 0 1)	Single	[0 0 1]
β–SiC	[37]	CVD	Si_2-H_6–C_2H_2–HCl	101.325	1423	145	Si(1 0 0) & Si(1 1 1)	Single & poly	[1 1 1]
β–SiC	[38]	CVD	HMDS[e] or TMS[f]	101.325	1173–1573	311 or 422	Si(1 0 0) & Si(1 1 1)	Single & poly	[1 1 1]
α–Si_3N_4	[18, 39]	CVD	NH_3–$SiCl_4$	0.007–0.040	1273–13273	126	Graphite	Amorphous & poly	[1 1 1]
α–Si_3N_4	[20]	CVD	NH_3–$SiCl_4$–C_3H_8	4.000–10.000	1373–1773	84–160	Graphite	Amorphous	
TiO_2 anatase	[40]	CVD	TTiP[g]–O_2	101.325	600–1300	120	Fused silica	Poly	[1 0 0]
BN	[28, 41]	CVD	BCl_3–NH_3	0.700–8.000	1473–2273	134	Graphite	Turbostratic	[0 0 1]
Graphite	[42–44]	CVD	C_3H_8	0.700–27.000	1618–2488	251	Graphite	Turbostratic	[0 0 1]

[a] PO, preferred orientation of deposit.
[b] CVD, chemical vapour deposition.
[c] MOCVD, metal–organic chemical vapour deposition.
[d] TMG, trimethyl gallium.
[e] HMDS, hexamethyldisilane.
[f] TMS, tetramethylsilane
[g] TTiP, titanium tetraisopropoxide.
[h] UHV, ultrahigh vacuum.
[i] RT, room temperature.

reaction, while PO is the preferred orientation of the deposit. Further details on these vapour deposited materials can be found in Appendix 1.

3. Results and discussion

Fig. 1 Shows a plot of the best current estimates of the normalized grain density versus burial parameter relation for Si, GaAs, SiC, Si_3N_4, TiO_2, BN and graphite (C). From this plot it can be seen that the normalized grain densities of these vapour deposited materials indeed increase as their corresponding burial parameters, β, increase. Moreover, lying on the left side of Fig. 1, where $\beta \ll 1$, are amorphous deposits, while the crystalline deposits lie on the right of the figure, where $\beta \gg 1$. It appears that two separate curves can be fitted to the crystalline data points in Fig. 1. These two curves are separately plotted in Figs 2 and 3. Although the amorphous data points exhibit considerable scatter, the general trend of a decrease in grain density as β decreases is still clear.

All data points in Fig. 1, except those pertaining to systems which possess a turbostratic ("layered") structure, i.e. BN(s) and graphite, are included in Fig. 2. These "non-layered" materials, which do not possess any turbostratic structure, seem to exhibit quite an abrupt decrease in their grain densities as they change from their crystalline state to their amorphous state. When $\beta > 1$, the grain densities of these "non-layered" materials remain at or very close to their theoretical single crystal density. As β becomes less than unity, these materials experience nearly a step decrease in their grain densities.

The resulting relationship between normalized grain density, $\mathscr{R}$, and β for turbostratic vapour deposited materials, i.e. BN(s), C(s), etc., is displayed in Fig. 3. Since none of the amorphous data used in this work belong to the family of turbostratic materials, it is assumed that there is only one general curve for

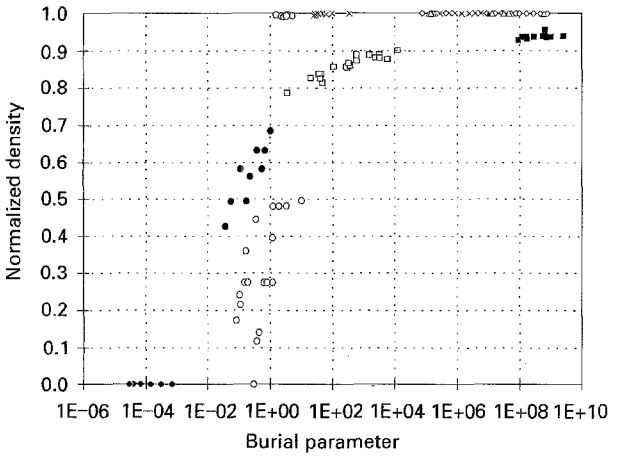

Figure 1 Correlation of the "observed" normalized grain densities (Equation 8) of some vapour deposited materials with the burial (escape) parameter, β, (Equation 1) estimated from deposition conditions (Table II) and material properties (Table I): (—) Si [9], (——) Si [32], (◇) Si [33], (◆) Si [34], (△) GaAs [35], (▲) GaAs [36], (+) SiC [37], (×) SiC [38], (○) Si_3N_4 [18, 39], (●) Si_3N_4 [20], (*) TiO_2 [40], (□) BN [28, 41], (■) C [42–44].

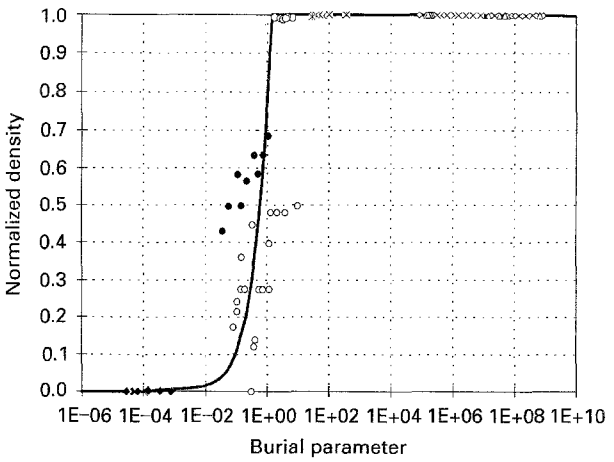

Figure 2 Correlation of the normalized grain densities of "non-layered" vapour-deposited materials with the burial (escape) parameter, β, (Equation 1) estimated from deposition conditions (Table II) and material properties (Table I): (—) Si [9], (——) Si [32], (◇) Si [33], (◆) Si [34], (△) GaAs [35], (▲) GaAs [36], (+) SiC [37], (×) SiC [38], (○) Si_3N_4 [18, 39], (●) Si_3N_4 [20], (*) TiO_2 [40].

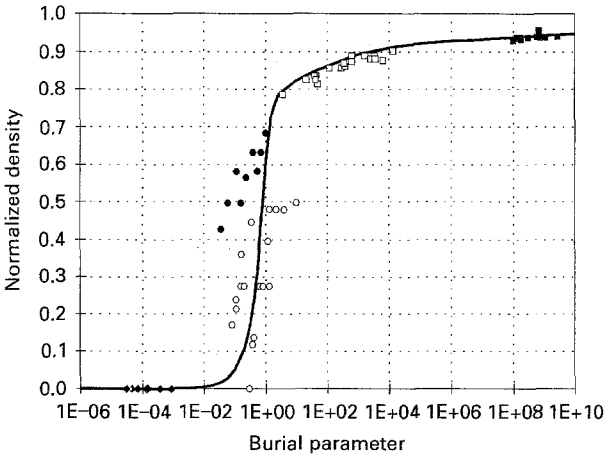

Figure 3 Correlation of the normalized grain densities of vapour-deposited materials having turbostratic ("layered") structure with the burial (escape) parameter, β, (Equation 1) estimated from deposition conditions (Table II) and material properties (Table I): (◆) Si [34], (○) Si_3N_4 [18, 39], (●) Si_3N_4 [20], (□) BN [28, 41], (■) C [42–44].

amorphous deposits, whether their crystalline counterparts exhibit a turbostratic structure [see Appendix 1, section on BN(s)] or not. As a result, the amorphous data points for the "non-layered" materials are also included in Fig. 3. From this figure, turbostratic materials exhibit a more gradual change in their grain densities as their burial parameters decrease (compared to the abovementioned more abrupt change observed in "non-layered" materials).

This difference in behaviour between turbostratic and "non-layered" materials may be explained by their relative ability to tolerate "lack-of-order" in their structure. In their crystalline state, "non-layered" materials must maintain co-ordination for their constituent atoms in all three dimensions. Once, this type of material loses order in one direction, its entire structure "collapses" and the material becomes structureless or amorphous. Hence, "non-layered"

materials would be expected to exhibit a more abrupt decrease in their grain densities as they change from their crystalline state to their amorphous state. On the other hand, turbostratic materials can tolerate the lack of three-dimensional co-ordination, as these materials retain order in only two-dimensions. Therefore, turbostratic materials exhibit a more gradual decrease in their grain densities as they change from being crystalline to being amorphous.

Recall that the activation energy for surface diffusion, ΔE_{SD}, of some of the vapour deposited materials tested in this work were actually estimated by setting β to be unity for deposits which are shown by XRD patterns to be in transition from their amorphous phase to their crystalline phase. One could argue that crystalline data points and amorphous data points which have their ΔE_{SD} estimated in this way, were forced to correspond to $\beta > 1$ and to $\beta < 1$, respectively. It cannot be denied that the greatest source of error in estimating the burial parameter originates from the values of ΔE_{SD} used. However, data with ΔE_{SD} not obtained by setting β to unity, but obtained from either the literature or from Dryburgh's model [4], also follow the trend of increase in grain density with increasing β. Moreover, these data obey the general pattern that amorphous deposits lie on the $\beta < 1$ side of an $\mathscr{R}(\beta)$ plot, while crystalline deposits lie on the $\beta > 1$ side of such a plot.

There will, of course, be other causes of "scatter" in the proposed correlation, some of which deal with the processes presumably "precluded" in the basic assumptions made earlier. Additionally, note that since β is a ratio of the successful arrival rate of depositing molecules to the surface diffusion rate of admolecules, it is very dependent on the actual prevailing deposit surface temperature. Incorrectly reported deposit surface temperatures will therefore lead to the prediction of incorrect β values, even if the parameter assignments (ν_0, ΔE_{SD}, etc.) are correct. Hence, some of the scatter of data points in Fig. 1 may be due to different degrees of accuracy in the deposit surface temperatures reported in the literature.

4. Conclusions

1. It is conjectured and demonstrated (using data for seven important materials) that the grain densities of vapour deposited materials are indeed determined principally by what has here been called the "burial" parameter (ratio of the mean time between successful impacts of depositing molecules on a unit cell area of the growing film to the mean time for an admolecule to surface diffuse to a lattice position). As expected from this universal normalized density versus burial parameter hypothesis, the reported grain densities increase as their associated burial escape parameters, β, increase; and they also obey the general trend that, for $\beta < 1$, the deposits formed are amorphous, while for $\beta > 1$, crystalline deposits are observed.

2. Actually, two types of relationship between the grain density and its associated β appear to be distinguishable (Figs 2 and 3). One trend involves turbostratic ("layered") materials such as BN(s), C(s), (Fig. 3), while the other involves materials which do not exhibit a "turbostratic" structure (Fig. 2). Evidently, the grain densities of turbostratic materials decrease more gradually as their corresponding β values decrease.

3. Some vapour deposition systems are evidently incapable of producing amorphous deposits, e.g. TiO_2(s) films grown from TTiP [40]. As made clear from the present vantage point, in such systems the reaction activation energies are such that rates of reaction and the rates of surface diffusion do not cross at a feasible temperature for amorphous films to deposit.

4. As a byproduct of this work, in the absence of more direct information, the activation energy for surface diffusion of admolecules on a growing deposit of "any" substance may be estimated by setting the burial parameter to unity for conditions corresponding to deposits shown by XRD patterns to be in transition between its amorphous and crystalline phase.

5. The simultaneous presence of homogeneous nucleation of microparticles in the vapour phase [6] causes changes in the grain density of deposits grown (*via* heterogeneous nucleation) on the substrate. The minimum density for CVD–graphite at some intermediate deposition temperature, attributed to the presence of gas phase reactions that produce soot [45] would cause these points to fall far from the present correlation.

Based on these encouraging findings, several recommendations are offered for future investigation:

1. It should be possible to introduce dimensionless time ratios other than the abovementioned burial parameter (Equation 1) to correlate/predict other vapour deposit properties of enegineering interest. Indeed, one such characteristic time ratio already in widespread use is the socalled Thiele modulus (ratio between the characteristic time for depositing molecules to diffuse through micropores in the substrate to the time for successful arrival of depositing molecules on the substrate surface), which dictates the ultimate porosity of vapour infiltrated deposits [46].

2. It is anticipated that the dimensionless ratio of the characteristic time for successful arrival of depositing molecules to the characteristic time for heterogeneous nucleation will be related to the number of monomers within each grain and hence, the grain size of any deposit. The validity of this hypothesis is being investigated by exploiting data from the literature and experimental data from the authors' own research group [40].

3. In addition to grain size and grain density, grain shape may also be necessary for predicting the bulk densities of vapour deposited materials.

Based on this line of reasoning, it seems likely that at least three different time–ratio parameters will be needed to predict the bulk densities of most vapour deposited materials. In any case, this approach to the ultimate development of rational, reasonably "universal" correlations between deposit quality and deposition conditions appears to be a promising one, worthy of further development.

Appendix 1

Silicon carbide

CVD–SiC(s) has a zincblende structure called β–SiC [16]. From Dryburgh's model, its ΔE_{SD} value was estimated as 2 eV (or 193 kJ mol^{-1}) [4].

Silicon nitride

Typical CVD–Si_3N_4(s) is α–Si_3N_4 which has a hexagonal structure [16]. Its minimum density was taken to be the lowest amorphous density reported by Niihara and Hirai [18] (2.6 g cm^{-3}). Using data published by Niihara and coworkers [18–20], ΔE_{SD} was estimated to be about 330 kJ mol^{-1}, by setting the burial parameter to be unity for deposits obtained in the transition regime between the amorphous and crystalline phase. When Hirai and Goto [20] repeated some of the experiments performed earlier by [18], different deposition patterns were observed. Hirai and Goto [20] attributed this difference to the uncorrected buoyancy effect which resulted in reduced deposition rates in the reactor of [18].

Titanium oxide

The crystal structure of CVD–TiO_2 films have been detected by XRD to be mainly anatase and rutile [40, 47]. The amorphous density for TiO_2 particles produced in a CVD tubular flow reactor was reported to be about 2.9×10^3 to 3.2×10^3 kg m^{-3} [23]. Since some of these particles were reported to be porous, the upper value of this range was taken as the minimum density for TiO_2 in this work. By observing the annealing behaviour of very thin amorphous film, ΔE_{SD} for TiO_2 anatase was estimated to be about 145 kJ mol^{-1} [21]. This value was confirmed by setting β to unity for published data of [25] and hence, was used in this work. Since only ΔE_{SD} for anatase TiO_2(s) is available, only anatase films were considered in this work.

The deposition of TiO_2(s) films via TTiP in an impinging jet CVD reactor from 600 to 1300 K at a total pressure of 1.013×10^5 Pa has been conducted in the authors' own research group [40]. Through XRD, it was found that these films were all polycrystalline. By assuming that the deposition rate in the heterogeneous reaction controlled regime is first-order, with an activation energy for reaction of about 120 kJ mol^{-1} [40], it was found that for the burial parameter to be unity, the corresponding deposition temperature must be near 375 K, which is much less than the minimum deposition temperature studied in the CVD system. Hence, it can be concluded that the rates of reaction and the rates of surface diffusion in the CVD system, do not cross at a feasible temperature for amorphous films to deposit.

Boron nitride

Depending on the deposition conditions, CVD–BN can be amorphous, turbostratic or hexagonal BN [26]. The structure of hexagonal boron nitride (h-BN) resembles that of graphite, in that it is made up of sheets of atoms in three-fold co-ordination. Turbostratic BN (t-BN) has two-dimensional order, but lacks three-dimensional co-ordination, perhaps best visualized as sheets of paper stacked randomly on top of one another. Consequently, the interlayer spacings of t-BN are larger than those of h-BN. These "extended" interlayer spacings in turbostratic materials translate to a slight, but noticeable, systematic change in their corresponding grain densities.

The amorphous density of BN does not appear to be available from the literature. In part because BN(s) and graphite are very similar in many aspects, the amorphous density of BN was assumed to be the same as that of amorphous carbon; about 1.5×10^3 kg m^{-3} [29]. ΔE_{SD} for BN(s) was estimated to be around 310 kJ mol^{-1} by setting β to be unity for deposits which are in transition between their amorphous and crystalline states [27, 28].

Graphite

Apart from its amorphous structure and its hexagonal structure (graphite), CVD–carbon also exhibits a turbostratic structure. The amorphous density for amorphous (glassy) carbon is about 1.5 g cm^{-3} [29]. Kürpick *et al.* [31] reported values ranging between 1 and 1.7 eV (96–164 kJ mol^{-1}) for the activation energy for desorption of CH, CD_4 and C_2H_2 from graphite single crystal surface [31]. These results were estimated by using four different methods from thermal desorption spectroscopy experiments. Since ΔE_{SD} of a material should be lower than its activation energy for desorption, ΔE_d, the lower value of the range reported for ΔE_d should represent a conservative upper bound for ΔE_{SD}. Hence, ΔE_{SD} of graphite is assumed to be 96 kJ mol^{-1} in this work.

Most of the graphite data published in the literature, including those used to test the burial parameter hypothesis in this work [42–44], exhibit a minimum in deposit density at some intermediate deposition temperatures. It was first shown by Diefendorf [45] that this minimum density could be eliminated if the gas phase reactions that produce soot are restricted by maintaining a low degree of saturation. Therefore, one can attribute this minimum density occurrence to the presence of gas phase reactions that produced soot. Consequently, data which correspond to this occurrence were omitted for testing the burial parameter hypothesis.

Hirai and Yajima [42] used resistance heating to supply the necessary energy for their CVD experiments. Harvey *et al.* [48] pointed out that when resistance heating of a rod is used, the inner regions of a 1 mm thick graphite deposit may be hotter than its surface by 200–400 °C (473–673 K) when the surface temperature is 2000 °C (2273 K). Hence, data on materials deposited at temperatures greater than 2000 °C (2273 K) were also omitted in this work.

Acknowledgements

This research was supported in part by US AFOSR (Grant AFOSR 91-0170), NASA–Lewis Research Center (Grant NAG 3-884) and motivated by our work on behalf of Advanced Ceramics Corporation (J. Shinko, M.B. Dowell, J. Lennartz, technical contacts). Special thanks are due to Dr Stanley Mroczkowski

(Yale, Department of Applied Physics), Dr Eric Altman (Yale, Department of Chemical Engineering), Roger E. Welser (Yale, Department of Applied Physics), Dr Robert Weber (Yale, Department of Chemical Engineering), Professor Victor Henrich (Yale, Department of Applied Physics) and Dr Suleyman A. Gökoğlu (NASA–Lewis Laboratories) for their helpful discussions, and also to Paul R. Bartholomew (Yale, Department of Geology) for assisting in the X-ray diffraction analysis of our TiO_2(s) films.

Added in proof

The "burial" parameter approach to correlating/predicting the degree of molecular disorder in deposits – and, hence, deposit density, has been quantified here for deposits grown from the vapour, with an explicit flux relation (Equation 2) valid for low density gases. Based on the comments of reviewers, however, two points should, perhaps, be made more explicitly:

First, in any particular deposition reactor there may be a rate-limiting diffusion boundary layer further from the growth interface, and the reagent vapour partial pressure in the feed may significantly exceed $p_{A,w}$ (see e.g., Ref. [1], pp 345–347). However, the resulting molecular flux would necessarily equal that across the (Knudsen-) sublayer adjacent to the surface. Thus, our deposit disorder correlation approach is not limited to interface-controlled, low density reactors.

Second, the underlying premise (regarding a "universal" connection between the "degree of amorphousness" in the deposit and the competition between surface diffusion and "burial") transcends the particular case of deposits grown from the vapour phase, explicitly addressed/quantified in this paper.

References

1. D. E. ROSNER, "Transport Processes in Chemically Reacting Flow Systems" (Butterworth-Heinemann, Stoneham, MA, 1986).
2. S. A. GÖKOĞLU, in "Proceedings of the 11th International Symposium on Chemical Vapor Deposition", Vol. 90–112, edited by K. E. Spear and G. W. Cullen (The Electrochemical Society, Pennington, NJ, 1990) p. 1.
3. C. HILL and S. JONES, in "Properties of Silicon", EMIS Data Reviews Series No. 4 (INSPEC, The Institution of Electrical Engineers, London, 1988) p. 935.
4. P. M. DRYBURGH, *J. Cryst. Growth* **87** (1988) 397.
5. W. A. TILLER, "The Science of Crystallization: Microscopic Interfacial Phenomena" (Cambridge University Press, 1991) p. 173.
6. D. E. ROSNER, J. COLLINS and J. L. CASTILLO, in "Proceedings of the 12th International Symposium on Chemical Vapor Deposition", Vol. 93–2, edited by K. F. Jensen and G. W. Cullen (The Electrochemical Society, Pennington, NJ, 1993) p. 41.
7. N. B. COLTHUP, in "Encyclopedia of Physical Science & Technology", Vol. 8, 2nd Edn, edited by R. A. Meyers (Academic Press) p. 106.
8. R. C. LORD, in "McGraw-Hill Encyclopedia of Science & Technology", Vol. 9, 6th Edn (McGraw-Hill) p. 162.
9. R. C. HENDERSON and R. F. HELM, *Surface Sci.* **30** (1972) 310.
10. R. W. G. WYCKOFF, "Crystal Structures" Vol. 1, 2nd Edn (Wiley, New York, 1963) p. 184.
11. Y. TATSUMI and H. OHSAKI, in "Properties of Silicon," EMIS Data Reviews Series No. 4 (INSPEC, Institution of Electrical Engineers, London, 1988) p. 3.
12. "Semiconductors: Group IV Elements and III–V Compounds, Data in Science and Technology", edited by O. Madelung (Springer-Verlag, Berlin, 1991).
13. J. A. VAN VECHTEN, in "Properties of Silicon", EMIS Data Reviews Series No. 4 (INSPEC, Institution of Electrical Engineers, London, 1988) p. 47.
14. G. B. STRINGFELLOW, "Organometallic Vapor-Phase Epitaxy: Theory and Practice" (Academic Press, 1989) p. 59.
15. T. NISHINAGA and K. I. CHO, *Jpn. J. Appl. Phys.* **130** (1988) 675.
16. F. S. GALASSO, "Chemical Vapor Deposited Materials" (CRC Press, 1991).
17. M. A. EI KHAKANI, M. CHAKER, A. JEAN , S. BOILY, J. C. KIEFFER, M. E. O'HERN, M. F. RAVET and R. ROUSSEAUX, *J. Mater. Res.* **9** (1994) 96.
18. K. NIIHARA and T. HIRAI, *J. Mater. Sci.* **11** (1976) 604.
19. P. L. LAUNER, "Silicon Compounds Register and Review, Petrarch Systems Silanes and Silicones" (Petrarch Systems, 1987).
20. T. HIRAI and T. GOTO, *J. Mater. Sci.* **16** (1981) 2877.
21. D. G. HOWITT and A. B. HARKER, *J. Mater. Res.* **2** (1987) 201.
22. R. H. PERRY and D. GREEN, "Perry's Chemical Engineers' Handbook", 6th Edn (McGraw-Hill, Singapore, 1984) pp. 3–23.
23. F. KIRKBIR and H. KOMIYAMA, *Can. J. Chem. Engng* **65** (1987) 759.
24. C. D. CRAVER (Ed.), "The Coblentz Society Desk Book of Infrared Spectra" (The Coblentz Society, 1977).
25. K. KAMATA, K. MARUYAMA, S. AMANO and H. FUKAZAWA, *J. Mater. Sci. Lett.* **9** (1990) 316.
26. R. T. PAINE and C. K. NARULA, *Chem. Rev.* **90** (1990) 73.
27. W. L. LEE, W. J. LACKEY and P. K. AGRAWA, *J. Amer. Ceram. Soc.* **74** (1991) 2642.
28. T. MATSUDA, N. UNO and H. NAKAE, *J. Mater. Sci.* **21** (1986) 649.
29. KIRK-OTHMER, "Encyclopedia of Chemical Technology" 3rd Edn (Wiley, New York).
30. K. SPEAR, *Earth Mineral Sci.* **56** (1987).
31. U. KÜRPICK, G. MEISTER and A. GOLDMANN, *Appl. Phys.* **A55** (1992) 529.
32. R. F. C. FARROW, *J. Electrochem. Soc. Solid-State Sci. Technol.* **121** (1974) 899.
33. J. BLOEM, *J. Cryst. Growth* **18** (1973) 70.
34. Y. TATSUMI, H. OHSAKI, Y. KURAHASHI, M. IIJIMA, K. KURUMI, K. MIURA and T. INO, *Jpn. J. Appl. Phys.* **25** (1986) 1152.
35. D. H. REED and S. K. GHANDHI, *J. Electrochem. Soc. Solid-State Sci. & Technol.* **130** (1983) 675.
36. D. W. SHAW, *J. Electrochem. Soc.* **115** (1968) 405.
37. S. NISHINO, K. TAKAHASHI, H. ISHIDA and J. SARAIE, in "Amorphous and Crystalline Silicon Carbide III", Vol. 56 (SPP, 1992) p. 295.
38. K. TAKAHASHI, S. NISHINO, J. SARAIE and K. HARADA, in "Amorphous and Crystalline Silicon Carbide IV", Vol. 71 (SPP, 1991) p. 78.
39. K. NIIHARA and T. HIRAI, *J. Mater. Sci.* **12** (1977) 1233.
40. J. COLLINS, PhD Thesis, Yale University (1994).
41. T. MATSUDA, H. NAKAE and T. HIRAI, *J. Mater. Sci.* **23** (1988) 509.
42. T. HIRAI and S. YAJIMA, *ibid.* **2** (1967) 18.
43. S. YAJIMA, T. SATOW and T. HIRAI, *J. Nuclear Mater.* **17** (1965) 116.
44. *Idem, ibid.* **17** (1965) 127.
45. D. F. DIEFENDORF, *J. Chimica Physica (Paris)* **57** (1960) 815.
46. T. M. BESSMAN, B. W. SHELDON, R. A. LOWDEN and D. P. STINTON, *Science* **253** (1991) 1104.
47. Y. TAKAHASHI, H. SUZUKI and M. NASU, *J. Chem. Soc., Faraday Trans. 1* **81** (1985) 3117.
48. J. HARVEY, D. CLARK and J. N. EASTBROOK, in "Special Ceramics", edited by P. Popper (Academic Press, New York, 1963) p. 183.

Received 8 April
and accepted 31 October 1994